

# Improved Maximum Entropy Analysis with an Extended Search Space

Alexander Rothkopf<sup>1</sup>

<sup>1</sup>*Fakultät für Physik, Universität Bielefeld, D-33615 Bielefeld, Germany*

(Dated: May 25, 2022)

## Abstract

We propose an improvement to the implementation of the well established Maximum Entropy Method by taking into account carefully the role of prior information. This involves a departure from Bryan's concept of search space, a change that becomes crucial for the success of the inversion task in case of e.g. small datasets or unreliable prior information. To adequately approach problems where an exponentially damped Kernel is used, we provide an implementation using the C/C++ language that utilizes high precision arithmetic adjustable at runtime [1]. The LBFGS algorithm is included in the code in order to attack problems without the need to resort to any search space restriction. An analysis of mock- as well as lattice QCD data is presented as illustration of the discussed issues.

## I. MOTIVATION

At the heart of the Maximum Entropy Method (MEM) lies the numerical optimization problem<sup>1</sup> of finding the maximum  $\rho^{\text{MEM}}$  of a functional  $P[\rho|D, I]$ , given input in the form of  $N_\tau$  data points  $D_i$  and  $N_\omega$  points  $m_l$  of prior information  $I$ . For fixed  $D$  and  $I$  this function  $P$  depends on  $N_\omega$  parameters  $\rho_l$ , the values of the test function  $\rho(\omega)$  at each discretized frequency step  $\omega_l$ .

In an effort to diminish the associated computational cost, the state of the art implementation resorts to the prescription of Bryan [3]. It restricts the optimization a priori to an  $N_\tau$  dimensional subspace, whose shape depends crucially on the prior information  $I$ .

In practice however we observe that contrary to the accepted train of thought, in general the global maximum of  $P[\rho|D, I]$  does not lie in the subspace of Bryan. In particular we find that it becomes necessary to supply already parts of the solution  $\rho^{\text{MEM}}(\omega)$  as the prior function  $m_l$  for Bryan's approach to reach the true global maximum. We will thus argue that Bryan's search space prescription relies on a fallacy regarding prior information and needs to be abandoned to reliably perform the MEM procedure. Since Bryan's central offer was a massive (but misleading) reduction of the degrees of freedom for the optimization process, we provide a systematic way to approach the correct global minimum by using an extended search space with  $N_{\text{d.o.f}} > N_\tau$ .

Let us make the above criticism clear with a simplistic example, which still captures all ingredients of the problem<sup>2</sup>. Assume we have a system characterized by the Kernel  $K(\tau, \omega) = \exp[-\omega\tau]$  and spectra  $\rho(\omega)$ , which contain only frequencies  $\omega \in [0, \omega_{\text{max}} = N_\omega\Delta\omega]$ . Assume further that we have a fixed number of almost ideal data points  $D^{\text{mock}}(\tau_i)$ ,  $\tau_i \in [0, ..N_\tau\Delta t]$  coming from the spectra. Then it follows that the  $N_\omega$  sized vectors  $u^i$  used in the construction  $\rho_l^{\text{B}} = m_l \exp[\sum_{i=1}^{N_\tau} b_i u_l^i]$  of the solution in Bryan's approach are already fixed. They are calculated as the column vectors of the matrix  $U$  arising in the Singular Value Decomposition (SVD) of the transpose of the kernel  $K^t = U\Sigma V$ . Since in Bryan's derivation there is no restriction on  $\omega_{\text{max}}$  we take it to be large compared to  $N_\tau\Delta t$ .

On the right of Fig.1 we show the vectors  $u_l^i$  from which the solution  $\rho^{\text{B}}$  is constructed.

<sup>1</sup> all definitions are given in the following section and many excellent reviews provide basic insight into the underlying concepts [2–5].

<sup>2</sup> Readers unfamiliar with MEM terminology can skip this part until having read through the introduction section.

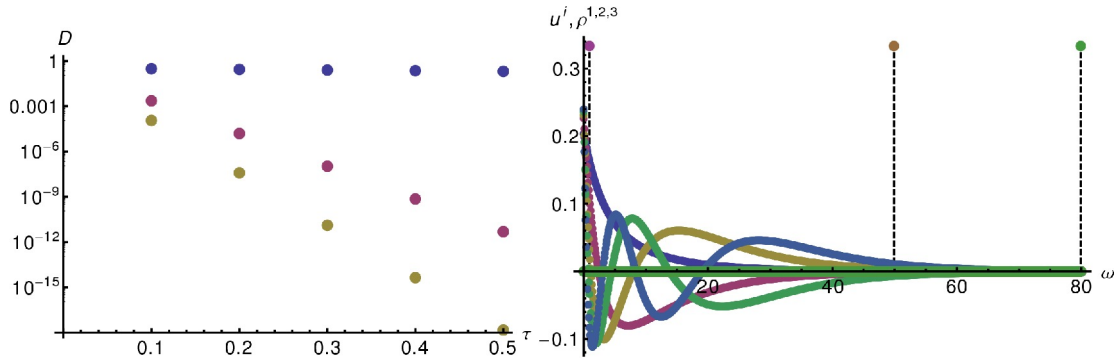


FIG. 1. Datasets of a fixed number of five points (left) for vastly different delta peak type functions  $\rho^{1,2,3}$  (right). Also shown on the right are the basis vectors  $u^i$  that span the singular subspace in Bryan’s prescription.

Please note that for  $\omega > 50$  there remains no oscillating structure. Using the same number of data points we can now encode vastly different (in this case delta peak like) spectra  $\rho^1, \rho^2, \rho^3$ , which are plotted in the same graph. Since we only changed the spectral information, i.e. the value of the data points  $D_i$ , Bryan’s prescription for the reconstruction does not change, i.e.  $N_\tau, N_\omega, \omega_{\max}$  and  $m_l$  are the same.

One can already see that from the structure of the singular subspace alone we only have a chance to reconstruct the lowest lying peak, since in the corresponding  $\omega$  range  $u^i(\omega)$  does possess some sort of peak structure. Since the basis functions become exponentially damped at  $\omega > 50$  there is no way to construct a linear combination of them to reach  $\rho^B \simeq \rho^2$  or  $\rho^B \simeq \rho^3$ . The only way how one is able to reproduce the data of the mock spectra  $\rho^{2,3}$  thus is by already including their features in the prior function  $m_l$ . In other words Bryan’s approach in general requires the prior information to already contain parts of the solution to be able to reproduce the provided data  $D_i$  successfully.

It is important to realize that if we were to vary  $\rho$  at each of the  $N_\omega$  points individually, i.e. step outside of Bryan’s search space, there is no problem in reproducing the mock data coming from the peaks in  $\rho^{2,3}$ , even if we do not know a priori of the existence of such structures.

After a brief introduction to the definitions and concepts of the MEM in section II, we will argue in section III that the problem illustrated in the above paragraphs arises from not taking into account the uncertainty present in the choice of prior information. We propose to expand Bryan’s search space systematically to approach the full search space

and in turn become able to find the correct global maximum. Sections IV and V present the application of our improved implementation to both mock data and real word data from lattice QCD simulations before ending with a brief conclusion.

## II. INTRODUCTION

### A. The general task

In the quantitative sciences one often encounters the task of reconstructing from a measured dataset a relevant quantity, whose values are not directly accessible through the used apparatus or method. In this paper we are interested in a class of problems where the relation between (ideal) data  $D$  and the (positive definite) function of interest  $\rho$  is given by an integral

$$D(\tau) = \int_{-\infty}^{\infty} K(\tau, \omega) \rho(\omega) d\omega \quad (1)$$

over a real-valued Kernel  $K(\tau, \omega)$ , which is known a priori. Depending on the form of the Kernel this ideal problem poses different kinds of difficulties. In case of a trigonometric function such as  $K(\omega, \tau) = \sin(\omega\tau)$  the inversion is related to the Fourier transformation, whereas in the case of  $K(\omega, \tau) = e^{-\omega\tau}$  a variant of the inverse Laplace transform has to be computed. The inverse Laplace transform in particular is known to be an ill-posed problem, since the rapid damping of the Kernel makes the data insensitive to details of  $\rho(\omega)$  at large values of the product  $\tau\omega$ .

Since our aim is to perform a numerical analysis on the data, we are obviously in need of a discretized version of Eq.(1). Discretization happens here on both sides, once in the  $\tau$  interval according to the available measurements and on the RHS in the choice of compact support for the integral over  $\omega$ . While the former is dictated by our experimental setup (or the results of a simulation algorithm), the latter corresponds to a choice that requires some prior information about the sought after function  $\rho(\omega)$  itself.

In the case of a Fourier transform, we know that

$$\omega_{\max} = \frac{2\pi}{\Delta t} \quad \text{and} \quad \Delta\omega = \frac{2\pi}{N\Delta t}. \quad (2)$$

Thus we use as a rule of thumb that the maximum frequency we can determine the function  $\rho$  at is restricted by how finely we sample the  $\tau$  interval and the available number of

points tells us how well we can resolve structures within the  $\omega$  interval. This information on the frequency side only tells us that the compact support of the integral in Eq.(1) needs to be chosen to a maximum of  $\omega_{\max}$  but does not further specify the actual relevant frequency range for our problem. We would need prior information to know where the function  $\rho(\omega)$  has non-vanishing contributions. With this in mind let us write

$$D(\tau_i) \simeq \int_{\omega_{\min}}^{\omega_{\max}} d\omega K(\tau_i, \omega) \rho(\omega) \simeq \sum_{l=0}^{N_\omega-1} K_{il} \rho_l \Delta\omega_l \quad (3)$$

Note that this expression does not constitute a simple linear problem since we are dealing with the additional constraint that the function  $\rho(\omega)$  has to be positive definite. Even if it were possible to sample the function  $D(\tau_i)$  at  $N_\omega$  points along the  $\tau$  interval, we cannot simply take the inverse of the, in that case, square Kernel matrix applied to  $D(\tau_i)$

In reality we are inevitably confronted with incomplete measurements in the sense that each data-point carries an error. This stems either from a necessarily imperfect measurement apparatus or stochastic simulation algorithm. Therefore the direct inversion of the problem described in Eq.(1) is even more complicated, since depending on the form of the kernel, noise can be amplified so strongly that it drowns any signal encoded in the data if a naive inversion of the problem is attempted.

## B. Bayesian inference

Here we briefly recount the most important aspects of the MEM procedure and refer the reader to the more concise literature [3–6] for most of the derivations. The issues relevant to our proposed improvement of the implementation of the MEM algorithm are discussed in detail.

In the case of an inversion problem, ill-posed due to the insensitivity of the Kernel on a particular  $\omega$  range and due to the fact that the data contains noise, there exist an infinite number of solutions  $\rho_i^{\chi^2}(\omega)$  that are compatible with the measured data  $D(\tau_i)$  *within the errors*  $\sigma(D(\tau_i))$ . It is therefore necessary to select from these possible solutions the one that is the most probable to describe the system under consideration. The term “probable” refers to our confidence that the obtained solution actually describes the system and as such contains a subjective element. If we have additional knowledge about the system beyond the measured data it will allow us to rule out some of the degenerate possibilities.

Therefore the answer to the question “what is the spectral function we are most confident in to describe the system” changes with the amount of prior knowledge available to us.

The mathematical approach to such questions of confidence is called inference[2]. In this paper we focus on the particular case of Bayesian inference, which derives its name from the theorem that underlies this formulation. Note that in the following, the term probabilities is used not in the frequentist sense, i.e. it is not restricted to describing the frequency of a certain outcome of a random variable over a large number of trials but pertains to the confidence of hypotheses.

Let us thus formally write for the probability of a test function  $\rho(\omega)$  to be the correct function to describe our system characterized by both data  $D(\tau_i)$  and further prior knowledge  $I$  as

$$P[\rho|D, I] = \frac{P[D|\rho] P[\rho|I] P[I|D, \rho]}{P[D|I] P[I|\rho]} \quad (4)$$

In the usual formulation of the Maximum Entropy method one assumes that the prior knowledge does not contain uncertainties, in which case  $P[I|\rho]$  and  $P[I|D, \rho]$  are just unity. (As we have seen in the introduction, the choice of  $\omega_{\min}$  and  $\omega_{\max}$  may already represent prior information that is not known with full certainty.) In the following we assume that all prior information is chosen to correctly characterize the system and write

$$P_{\text{MEM}}[\rho|D, I] = \frac{P[D|\rho] P[\rho|I]}{P[D|I]} \quad (5)$$

Our task will be to find the test function that maximizes Eq.(5), i.e. a  $\rho^{\text{MEM}}(\omega)$  that fulfills

$$\left. \frac{\delta}{\delta\rho} P_{\text{MEM}}[\rho|D, I] \right|_{\rho=\rho^{\text{MEM}}} = 0 \quad (6)$$

The RHS of Eq.(5) contains two terms that depend on the function  $\rho(\omega)$  and which are thus of interest in the search for an extremum of the LHS ( $P[D|I]$  is understood as a normalization factor). The first is called the Likelihood  $P[D|\rho]$ , which characterizes how well the test function reproduces the measured data and the second one,  $P[\rho|I]$ , denotes the prior probability, which tells us how well the test function obeys the constraints set by our prior knowledge [3–6].

### C. Likelihood

Let us consider the case where one samples a real function  $D(\tau)$  over an interval  $\tau \in [0; \beta]$  at  $N_\tau$  not necessarily equidistant data-points  $\tau_i$ , with  $N_c$  repetitions of the measurement. Each of the individual values  $D^k(\tau_i)$  can be used to calculate an average

$$D_i = D(\tau_i) = \frac{1}{N_c} \sum_{k=0}^{N_c-1} D^k(\tau_i) \quad (7)$$

and an estimate of the associated error to this the average value in form of the correlation matrix

$$C_{ij} = \frac{1}{N_c(N_c - 1)} \sum_{k=0}^{N_c-1} (D_i^k - D_i)(D_j^k - D_j)$$

This matrix contains the variance of the measurements on its diagonal but furthermore provides important off-diagonal components that describe correlations in the data between at the different  $\tau_i$ 's.

Let us assume the the  $N_c$  measurements  $D_i^k$  we perform to create the average  $D_i$  at step  $\tau_i$  are a sampling from a random variable [4] with an unknown probability distribution  $P[D|\rho]$  determined by the correct but unknown  $\rho$ . We can write down the corresponding joint probability density function

$$P[D^0, D^1, \dots, D^{N_c-1}|\rho] = P[D^0|\rho]P[D^1|\rho] \dots P[D^{N_c-1}|\rho] \quad (8)$$

where  $\rho$  is fixed and the measured values are seen as parameters. Since we however would like to estimate  $\rho$  itself from the given data, we can turn this relation on its head and look for the probability of the data given a test function  $\rho$  instead. The central limit theorem then tells us that in the case of performing a large number of measurements the likelihood can be written as a Gaussian (an assumption, which should be checked for a small number of measurements)

$$P[D|\rho] \propto e^{-\mathcal{L}} \quad (9)$$

$$\mathcal{L} = \sum_{i,j=0}^{N_\tau-1} (D_i - D_i^\rho)[C^{-1}]_{ij}(D_j - D_j^\rho) \quad (10)$$

Here  $D^\rho$  denotes the data one obtains by inserting the current test function  $\rho$  into Eq.(3).

Note that the expression for  $\mathcal{L}$  corresponds to the least squares distance between measured data and model data. This reminds us that the  $\chi^2$  fitting method is based on the notion of maximum Likelihood and corresponds to setting the the prior probability constant in Eq.(5).

The double sum in Eq.(10) can be avoided by transforming both measured data and the corresponding Kernel to a basis  $R$  in which the correlation matrix is diagonal  $\text{diag}[\sigma_i^2] = R^{-1}CR$ , i.e.

$$\tilde{K} = R^{-1}K, \quad \tilde{D} = R^{-1}D \quad (11)$$

and hence the Likelihood function takes the simpler form

$$\mathcal{L} = \frac{1}{2} \sum_{i=0}^{N_\tau-1} \frac{1}{\sigma_i^2} \left( \tilde{D}_i - \sum_{j=0}^{N_\omega-1} \tilde{K}_{ij} \rho_j \right)^2 \quad (12)$$

#### D. Prior Probability

The goal of including a non-constant prior probability is to regularize the ill-defined  $\chi^2$  fitting procedure of maximizing the likelihood probability. Making explicit all our assumptions and additional knowledge about the system at hand is what allows us to do so. To encode such prior knowledge one defines a function  $m(\omega)$ , which is interpreted as a realization of the correct function  $\rho(\omega)$  if our prior knowledge  $I[m(\omega)]$  were to fully characterize the system. Since we only have prior knowledge in a certain  $\omega$  range (otherwise we would have already known the correct function  $\rho$ ) the support of this function is

$$\Omega = \left\{ \omega \mid \mathbb{P}\left[I[m(\omega)] \mid D, \rho\right] = 1 \right\} \quad (13)$$

If we then ask for a functional that regularizes the task of estimating  $N_\omega$  parameters in  $\rho$  from  $N_\tau$  data-points without introducing any additional structures that are not encoded in our data while fulfilling the constraints of the prior knowledge, one is lead to the concept of relative entropy [4] derived by Shannon and Janes

$$\mathbb{P}[\rho \mid I(m)] \propto e^{\alpha \mathcal{S}} \quad (14)$$

$$\alpha \mathcal{S} = \alpha \int_{\Omega} \left[ \rho(\omega) - m(\omega) - \rho(\omega) \log \left( \frac{\rho(\omega)}{m(\omega)} \right) \right] d\omega \quad (15)$$

This expression differs from the usual prescription in which the support  $\Omega$  is taken to span the whole frequency range.

Let us recall that one performs a numerical inversion of Eq.(1) because there does not exist an analytic expression for or even a perturbative approximation to the true answer  $\rho^{\text{MEM}}(\omega)$  for most of the  $\omega \in [\omega_{\min}, \omega_{\max}]$ . Therefore the measured data should contain information on features of the spectral function that we cannot fully anticipate, i.e we do not have firm prior knowledge about. If we however choose the function  $m(\omega)$  to span over the whole frequency range we implicitly make the false assumption that we have prior information which constraints the spectral function to the shape of  $m(\omega)$  even at  $\omega$  where the data will clearly introduce unknown features. If we make such a choice of  $\Omega = [\omega_{\min}, \omega_{\max}]$  we need to put into the function  $m(\omega)$  already the correct spectral function from the beginning to comply with  $P[I|D, \rho] = 1$ .

The hidden assumption in the common implementation of the MEM is that the data carries small enough noise to constrain the spectrum well enough in the region where correct prior information is absent. Then we can push ahead and extend the support  $\Omega$  of  $m(\omega)$  to the whole frequency range and write [3–6]:

$$\alpha \mathcal{S} \simeq \alpha \sum_{l=0}^{N_{\omega}-1} \left[ \rho_l - m_l - \rho_l \log \left( \frac{\rho_l}{m_l} \right) \right] \Delta \omega_l \quad (16)$$

Note that we have introduced a weighting factor  $\alpha$  on the LHS, which will allow us to evaluate the Eq.(5) for different strengths of the regularization. In the final result this parameter is marginalized self consistently using Bayes theorem and thus does not enter our solution.

The choice of the function  $m(\omega)$  itself and the dependence of the final result can be used as a measure to distinguish which features are actually constrained by the data and which are introduced by to our choice of prior function as discussed in subsection III D.

### III. MEM WITH AN EXTENDED SEARCH SPACE

As we have seen, the MEM procedure asks us to find the global maximum of Eq.(5) in terms of a test function  $\rho$ . Using the explicit expressions for the likelihood and prior

probability we have

$$P_{\text{MEM}}[\rho|D, I(\mathbf{m})] \propto \exp \left[ \mathcal{Q}^\alpha[D, \rho, I(\mathbf{m})] \right] = \exp \left[ \alpha \mathcal{S}[\rho, I(\mathbf{m})] - \mathcal{L}[\rho, D] \right] \quad (17)$$

The real exponential is a monotonous function in its argument, hence we can look for the extremum of the function  $\mathcal{Q}$  instead<sup>3</sup>

$$\left. \frac{\delta}{\delta \rho} \mathcal{Q}^\alpha \right|_{\rho=\rho^\alpha} = 0 \quad (18)$$

At this point we would like to remind the reader that the function  $\rho$  is discretized at  $N_\omega$  points along the frequency direction. Even if the number of provided data points is small  $N_\tau \ll N_\omega$  it is possible to show that  $\mathcal{Q}^\alpha(\rho)$  has a unique maximum if it exists [5]. This is possible since we provide through the function  $\mathbf{m}(\omega)$  an additional  $N_\omega$  points of information to constrain the final outcome. The proof only relies on the particular form of  $\mathcal{L}$  and  $\mathcal{S}$  and does not presume any particular parametrization of the solution. Therefore even using all  $N_\omega$  degrees of freedom to search for the maximum of  $\mathcal{Q}^\alpha(\rho)$  will lead to a unique answer if the maximum exists.

#### A. Solution for a given regularization $\alpha$

Since we are interested in resolving the function  $\rho^{\text{MEM}}(\omega)$  with a large number of points along the frequency axis, this task is computationally demanding. As an example, the popular Levenberg Marquardt routine (LM) requires an inversion of the Hessian matrix, which scales with  $\mathcal{O}(N_\omega^3)$  and thus quickly becomes too costly. Approximate algorithms such as BFGS or its variant LBFGS, that approximate the Hessian iteratively can reduce the computational cost in the cases where  $N_\omega$  is too large for the application of LM[7]. Optimizing in a very high dimensional search space however, will often encounter degenerate local minima, in which the algorithm will spend appreciable amounts of time and sometimes even settles down. It is therefore in the interest of economy to find ways in which we can constrain the search space a priori.

The established approach by Bryan is to ask in what subspace of the search manifold we can expect the solution of our problem to lie and then to restrict the whole search to

---

<sup>3</sup> Since many numerical algorithms are geared toward finding the minimum of a function one often uses  $-\mathcal{Q}$  in the actual computation.

this subspace. First of all this approach bears the intrinsic danger that the sub-manifold defined from the final result is not connected so that when starting from a randomly chosen position we have no proof whether we will be able to reach the correct extremum. In addition the use of the assumption that there is no uncertainty in the prior function  $m(\omega)$  will lead to the conclusion that the MEM spectral function is located in a subspace given by the image of the linear transformation  $K^t$ .

The starting point for our approach is the observation that the global maximum of the  $Q$  functional of Eq.(17) in general lies outside of the singular subspace proposed by Bryan. We have illustrated this point in the motivation section at the beginning of this paper and will give explicit examples based on mock data in the next section. We observe in particular that without a special choice of prior function the basis functions that span Bryan's singular subspace often do not include the features that are encoded in our data. If one remains within Bryan's prescription this can lead to the apparent necessity to supply additional model information, such as peaks at certain frequencies, into the prior function for a successful reconstruction even though the data encodes such information itself.

Hence we set out to find the inconsistency in the definition of the singular subspace. Inserting  $Q^\alpha$  from Eq.(17) into the stationary condition Eq.(18) we arrive at the following expression for the solution  $\rho^\alpha(\omega)$ :

$$-\alpha \log \left[ \frac{\rho^\alpha(\omega)}{m(\omega)} \right] = \int d\tau' \frac{\delta D^\rho(\tau')}{\delta \rho(\omega)} \frac{\delta \mathcal{L}[D, D^\rho]}{\delta D^\rho(\tau')} \quad \forall \omega \in \left\{ \omega \mid P[I[m(\omega)] | D, \rho] = 1 \right\} \quad (19)$$

Obviously the applicable  $\omega$ 's do not span the full frequency range, otherwise we already knew the complete answer of the inversion. Let us continue with this expression in discretized form

$$\alpha \log \left[ \frac{\rho_l^\alpha}{m_l} \right] = \sum_{i=0}^{N_\tau-1} \tilde{K}_{il} \frac{\delta \mathcal{L}[D, D^\rho]}{\delta D_i^\rho} \quad (20)$$

If we follow Bryan's suggestion and deploy the Singular Value Decomposition (SVD) for the transpose we get

$$[K^t]_{ij} = U_{ik} \Sigma_k [V^t]_{kj} \quad (21)$$

Here  $U$  denotes an orthogonal  $N_\omega \times N_\tau$  matrix,  $\Sigma$  are the  $N_\tau$  singular values and  $V^t$  represents a square  $N_\tau \times N_\tau$  orthogonal matrix. In order to make the following argument clear,

we let Eq.(20) guide us in expressing the solution  $\rho_l^\alpha$  in a different parametrization that already encodes positive definiteness (i.e. it is not the prior function itself that enforces this condition)

$$\rho_l^\alpha = m_l \exp[\tilde{\rho}_l] \quad (22)$$

Inserting back into Eq.(20) gives

$$-\alpha \tilde{\rho}_l = \sum_{i=0}^{N_\tau-1} K_{il} \frac{\delta \mathcal{L}[\mathcal{D}, \mathcal{D}^\rho]}{\delta \mathcal{D}_i^\rho} \quad (23)$$

which tells us that the  $l$ th entry of the vector  $\tilde{\rho}$  can be determined through the corresponding row of the linear transformation  $\hat{K}^t$  and thus can be constructed from the  $N_\tau$  parameters  $\tilde{b}_i$  that multiply the columns  $u$  of the matrix  $U$ .

$$\rho_l^\alpha = m_l \exp \left[ \sum_{i=0}^{N_\tau-1} u_{li} \tilde{b}_i \right] \quad (24)$$

We can now clearly see where the inconsistency arises. If we were to forget that the range of applicable frequencies is restricted as shown in Eq.(19), it appears that the spectral function can be located in the image of the linear transformation  $K^t$  at all  $\omega$ . Once restricted to this subspace we implicitly assume that the prior function already encodes the correct spectrum. Since we usually only provide a prior function that reproduces the sought after function  $\rho$  in a particular  $\omega$  range it is understandable why in some cases the maximization of  $\mathcal{Q}$  fails completely in Bryan's singular subspace and in other cases succeeds only after an explicit inclusion of model features in the prior function.

In general one cannot define a simple overall search space that will contain the solution for all  $\omega$ . If we restrict ourselves to Bryan's subspace we perform an ad-hoc selection of basis functions to compose the test function  $\rho(\omega)$  out of. Usually this corresponds to an artificial smoothing of the solution. Depending on the features encoded in the data the true solution can lie very close to Bryan's subspace in which case the established approach yields satisfactory results. This however needs to be checked in each analysis. (An example where Bryan's search space will come to its limits are functions  $\rho(\omega)$  that are composed solely from many finely spaced delta peaks.)

## B. Systematic extension of the search space

In the previous subsection we have seen that in order to correctly treat the inclusion of prior information into the MEM analysis, we have to depart from Bryan’s search space prescription. Even though there is no general closed form of the solution manifold available, it is possible to systematically increase Bryan’s subspace to approach the full search space. To this end we propose applying the SVD to the transpose of a Kernel  $K_{\text{ext}}$  that is constructed in a way as if more data-points were available, i.e using a  $\tau$  interval divided by  $N^{\text{ext}} > N_\tau$  steps. The resulting matrix  $\bar{U}$

$$(K_{\text{ext}}^t)_{i,j} = \bar{U}_{ik} \bar{\Sigma}_k [\bar{V}^t]_{kj} \quad (25)$$

then contains the extended search space basis, from which to construct the test function, parametrized by  $N^{\text{ext}}$  parameters  $b_i$

$$\rho_l = m_l \exp \left[ \sum_i \bar{u}_{li} b_i \right] \quad (26)$$

In practice we have found the following recipe to be useful: Starting with Bryan’s search space one increases  $N^{\text{ext}}$  until the value of  $Q$  does not decrease significantly anymore.

One finds that including more and more basis vectors will lead to an increase of “wiggly” features in the reconstructed function that are not constrained by the data and which must be identified as such by performing an systematic error analysis through varying the prior function as discussed in subsection III D.

Note also that progress in the mathematics of optimization problems, e.g the development of the (L-)BFGS [7] algorithm, allows us to perform a minimization of the functional  $Q^\alpha$  directly with a test function that is sampled at  $N_\omega \sim \mathcal{O}(1000)$  points. This approach is sound in principle but in practice we have found it to be sometimes impeded by the many small local extrema that it encounters on its way to the global extremum.

### C. Self consistent averaging over $\alpha$

After having obtained solutions for different regularizations  $\alpha$ , we can self consistently marginalize the dependence on this parameter[3–6] using the following relation

$$\rho^{\text{MEM}}(\omega) = \int \mathcal{D}\rho \int d\alpha \rho(\omega) P[\rho|D, I(m), \alpha] P[\alpha|D, I(m)] \quad (27)$$

$$\simeq \int d\alpha \rho^\alpha(\omega) P[\alpha|D, I(m)] \quad (28)$$

The explicit expression of  $P[\alpha|D, I(m)]$  has been shown to be

$$P[\alpha|D, I(m)] \propto \exp \left[ \mathcal{Q}[D, \rho^\alpha, I(m)] + \frac{1}{2} \sum_{k=0}^{N_\tau-1} \log \left( \frac{\alpha}{\alpha + \Delta\omega \lambda_k} \right) \right] \quad (29)$$

where  $\lambda_k$  are the  $N_\tau$  non-zero eigenvalues of the matrix

$$\Lambda_{ij}^\alpha = \sqrt{\rho_i^\alpha} \left. \frac{\delta^2 L}{\delta \rho_i \delta \rho_j} \right|_{\rho=\rho^\alpha} \sqrt{\rho_i^\alpha} \quad (30)$$

Let us see why this symmetric  $N_\omega \times N_\omega$  matrix only contains such a small number of nonzero eigenvalues. Using the Singular Value Decomposition of  $K^t$  (this is the Kernel of Eq.(3) with  $N_\tau$  steps along the  $\tau$  axis) in Eq.(21) we can rewrite ( $\sqrt{\rho^\alpha}$  denotes the vector obtained after applying the square root to each individual component  $\rho_i^\alpha$ )

$$\Lambda^\alpha = \sqrt{\rho^\alpha} \mathbf{U} \Sigma \mathbf{V}^t \left. \frac{\delta^2 L}{\delta D^\rho \delta D^\rho} \right|_{\rho=\rho^\alpha} \mathbf{V} \Sigma \mathbf{U}^t \sqrt{\rho^\alpha}. \quad (31)$$

With the additional definition of the two symmetric  $N_\tau \times N_\tau$  matrices

$$\mathbf{M} = \Sigma \mathbf{V}^t \left. \frac{\delta^2 L}{\delta D^\rho \delta D^\rho} \right|_{\rho=\rho^\alpha} \mathbf{V} \Sigma \quad (32)$$

$$\mathbf{T} = \mathbf{U}^t \text{diag}[\rho] \mathbf{U} \quad (33)$$

and an application of Sylvester's determinant theorem we can rewrite the Eigenvalue equation for the matrix  $\Lambda$  as

$$0 = \det \left[ \Lambda - \lambda_k \mathbf{I}_{N_\omega \times N_\omega} \right] \quad (34)$$

$$= \det \left[ \sqrt{\rho^\alpha} \mathbf{U} \Sigma \mathbf{V}^t \left. \frac{\delta^2 L}{\delta D^\rho \delta D^\rho} \right|_{\rho=\rho^\alpha} \mathbf{V} \Sigma \mathbf{U}^t \sqrt{\rho^\alpha} - \lambda_k \mathbf{I}_{N_\omega \times N_\omega} \right] \quad (35)$$

$$= \det \left[ \Sigma \mathbf{V}^t \left. \frac{\delta^2 L}{\delta D^\rho \delta D^\rho} \right|_{\rho=\rho^\alpha} \mathbf{V} \Sigma \mathbf{U}^t \sqrt{\rho^\alpha} \sqrt{\rho^\alpha} \mathbf{U} - \lambda_k \mathbf{I}_{N_\tau \times N_\tau} \right] \quad (36)$$

$$= \det \left[ \mathbf{M} \mathbf{T} - \lambda_k \mathbf{I}_{N_\tau \times N_\tau} \right] \quad (37)$$

Here it is important to note that the product of two symmetric matrices is not necessarily symmetric, i.e.  $MT \neq TM$ , so that algorithms for hermitian matrices cannot be used. Of course, since the spectrum of the original matrix  $\Lambda$  is real, the matrix  $MT$  does not harbor any complex eigenvalues. In addition we see that the matrix  $\Lambda$  contains two factors of the Kernel  $K$ , which, in the case of a large dynamical range in  $K$ , requires arithmetic of around twice the precision compared to the rest of the procedure to yield correct values.

The reader should also be aware that the above manipulations are independent from our choice of search space. The matrix  $\Lambda$  always has  $N_\tau$  non-zero eigenvalues even if we choose a search space with a different dimensionality. Furthermore we note that if one artificially restricts the SVD space by taking only a number of singular values larger than a certain small value into account, one has to ensure that the corresponding eigenvalues of the Matrix  $\Lambda$  that one discards are small in comparison to the values  $\alpha$ .

#### D. Error estimation

The estimation of statistical and systematic errors is an essential part of every MEM analysis. Two of the error estimation method to be discussed below require the analysis to be repeated several times under different circumstances. In practice it is important to check whether the minimization routines successfully converged to an extremum at each of the different runs. If a single run fails and is not detected (in case one uses automated scripts) the whole error estimation will be contaminated.

##### 1. Statistical errors

The statistical error of the reconstructed function  $\rho^{\text{MEM}}(\omega)$  is directly related to the quality of the supplied data. The larger the uncertainty in  $D_i$ , the more possible degenerate solutions there exist from which the MEM has to pick a single one due to our prior knowledge. (Remember that we use the assumption that the data will always constrain the spectrum strongly enough to overpower our incorrect use of the prior function in Eq.(16).)

A straight forward way is to use resampling, such as the blocked Jackknife method, where the full MEM procedure is carried out  $N_J$  times on subsets of the data, where each

time a different block of  $N_c/N_J$  measurements is removed. The individual results  $\rho_i^J(\omega)$  are then averaged and the Jackknife variance is calculated as

$$\rho^J(\omega) = \frac{1}{N_J} \sum_{i=0}^{N_J-1} \rho_i^J(\omega) \quad (38)$$

$$(\sigma^J)^2 = \frac{N_J-1}{N_J} \sum_{i=0}^{N_J-1} \left( \rho^J(\omega) - \rho_i^J(\omega) \right)^2 \quad (39)$$

## 2. Systematic Errors

We can distinguish two types of systematic error, the first pertains to the goodness of fit achieved by the minimizer and the other to the confidence we can place in structures of  $\rho$  to actually be encoded by the data.

The former can be approximated by the curvature of the  $\mathcal{Q}$  functional at the solution  $\rho^\alpha$  for each value of  $\alpha$  (the final error is then also averaged over the probability distribution for  $\alpha$ ). This concept of error is usually applied to intervals of finite length along the frequency axis.

$$\langle (\sigma_\alpha^{\text{GF}})^2 \rangle_{I_i} = \frac{1}{\omega_{i+1} - \omega_i} \int_{\omega_i}^{\omega_{i+1}} \int_{\omega_i}^{\omega_{i+1}} d\omega d\omega' \left( \frac{\delta^2 \mathcal{Q}}{\delta \rho(\omega) \delta \rho(\omega')} \right)^{-1} \Big|_{\rho=\rho^\alpha} \quad (40)$$

$$\langle (\sigma^{\text{GF}})^2 \rangle_{I_i} = \int d\alpha (\sigma_{\alpha,i}^{\text{GF}})^2 P[\alpha|D, I(m)] \quad (41)$$

Note that the determination of the errors is completely independent from the actual search for the extremum of the functional  $\mathcal{Q}$ . Since the above formula includes the inversion of a  $N_\omega \times N_\omega$  sized matrix it can become a bottleneck in the performance of the MEM code as the inversion has to be carried out for each value of  $\alpha$ . For a speed up, we can choose not to invert the full error matrix but instead only the submatrix over which we perform the integration of the current subinterval  $[\omega_i, \omega_{i+1}]$ . In the next section we present a comparison between the errors found from the full inversion and the approximation.

The remaining test of confidence in our result is done simply by varying the shape (or more naively just the amplitude) of the prior function  $m(\omega)$   $N_p$  times, over an interval that is as large as possible without introducing numerical instabilities in the reconstruction. Any structure in the resulting  $\rho_i^m$ 's that is determined with high confidence by the data will not be susceptible to the changes. Any other structure is fixed primarily by our

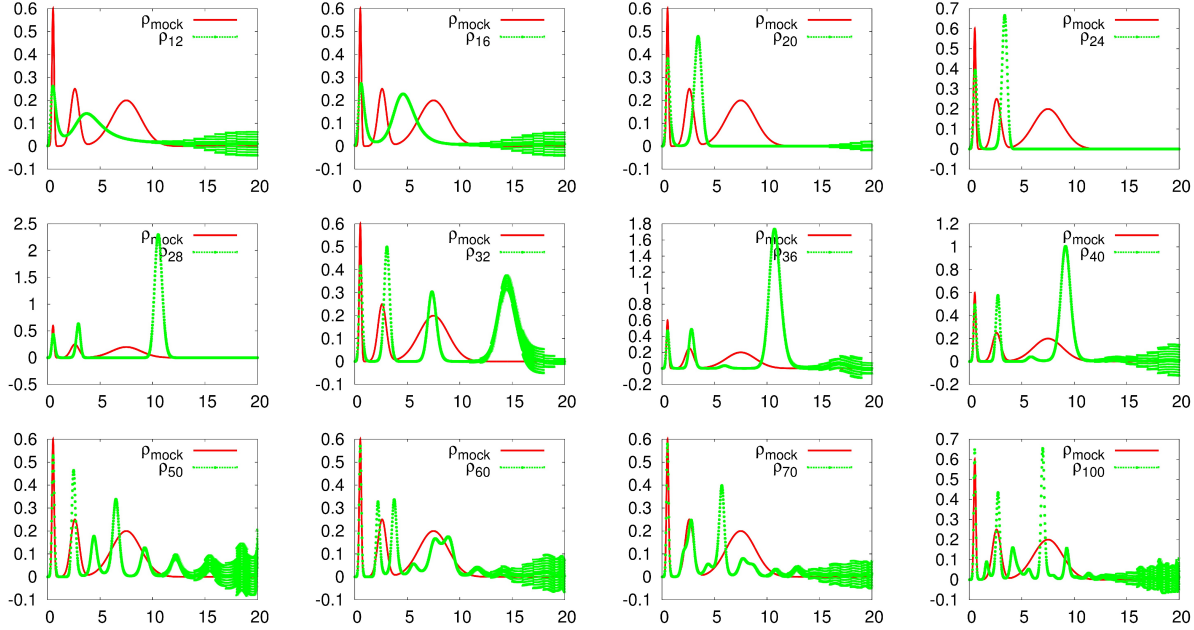


FIG. 2. Reconstruction of the mock function  $\rho_{\text{mock}}$  for different values of  $N^{\text{ext}}$ . Negative frequency structures are too small to see and are thus shown separately in Fig.3

choice of prior input and thus will show variation under change of the prior function. Since this approach is not based on a statistical propagation of errors we use the (somewhat arbitrary) convention that the error should be taken as the largest deviation from the average found in the different runs:

$$\rho^m(\omega) = \frac{1}{N_p} \sum_{i=0}^{N_p-1} \rho_i^m(\omega) \quad (42)$$

$$(\sigma^m)^2 = \max_i \left| \rho^m(\omega) - \rho_i^m(\omega) \right| \quad (43)$$

#### IV. MOCK DATA ANALYSIS

In order to illustrate the arguments made in the previous sections we perform a mock data analysis, where the MEM algorithm with an exponentially damped Kernel

$$K(\tau, \omega) = \exp[-\tau\omega] \quad (44)$$

is used to reconstruct an a priori known function  $\rho^{\text{mock}}$ . The mock function is given as an analytical expression constructed from a sum of four Gaussian peaks with parameters

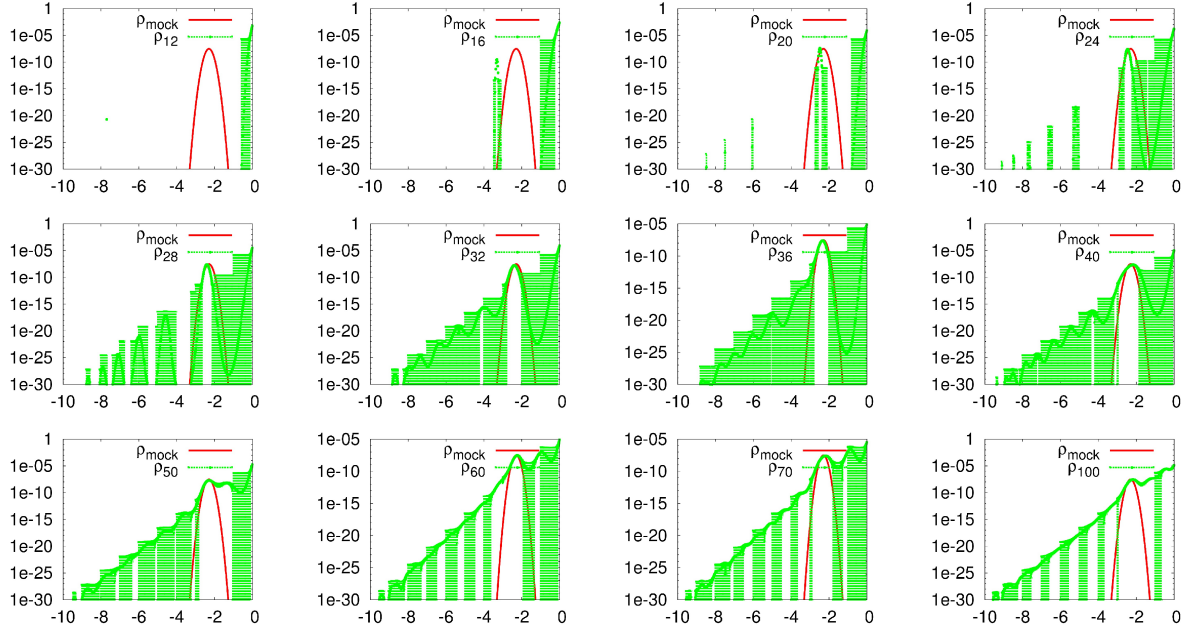


FIG. 3. The negative frequency part of the reconstructions of the mock function  $\rho_{\text{mock}}$  for different values of  $N^{\text{ext}}$

shown in Tab.I. From it a noisy set of data-points is generated and fed to the MEM code. We use  $N_{\omega}^{\text{mock}} = 5000$  to construct ideal data  $D^{\text{ideal}}$ , which is subsequently distorted by

	1st Peak	2nd Peak	3rd Peak	4th peak
Amplitude:	$3e^{-8}$	0.6	0.25	0.2
Position:	-2.3	0.52	2.6	7.5
Width:	0.1	0.1	0.4	1.4

TABLE I. Parameters of the Gaussian peaks used in the mock function  $\rho_{\text{mock}}$

Gaussian noise at each individual  $\tau_i$  with variance  $\delta D_i^{\text{mock}}$ , its strength controlled by the parameter  $\eta$ :

$$\delta D_j^{\text{mock}} = j\eta D_j^{\text{ideal}}, \quad j \in [1, \dots, N_{\tau}] \quad (45)$$

We choose as prior the function

$$m(\omega) = \frac{1}{\omega + \omega_0}$$

even though the original spectral function did not in fact contain such a high frequency behavior. This choice helps us to separate the features encoded in the data from any

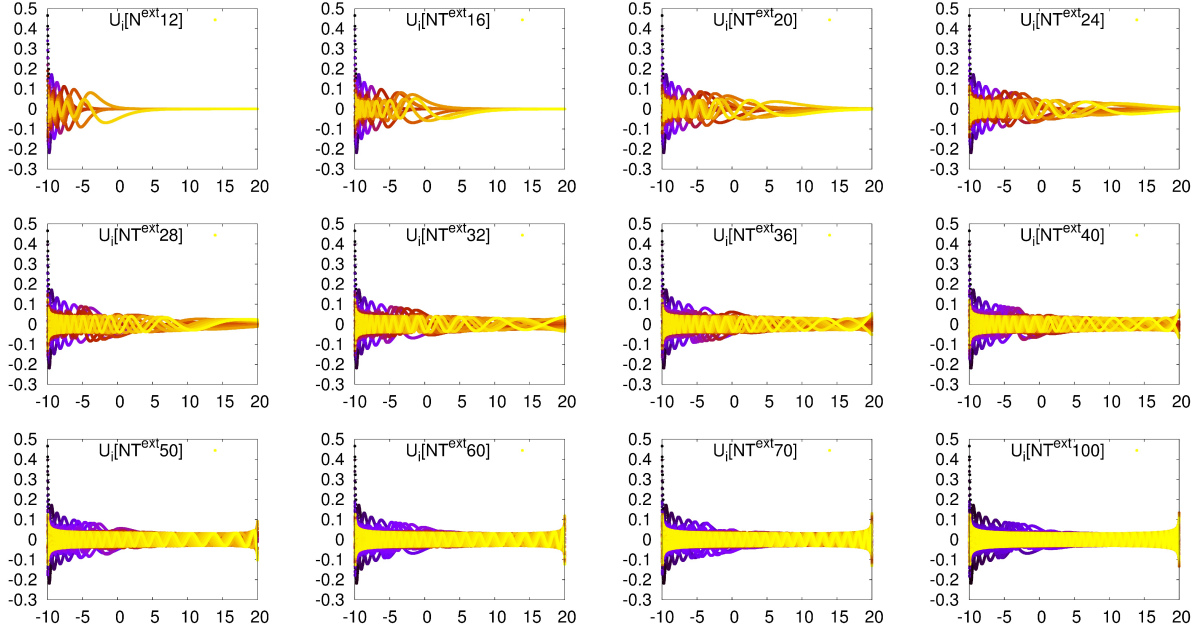


FIG. 4. Basis vectors of the search space for different values of  $N^{\text{ext}}$

artificial structures introduced through our choice of  $m(\omega)$  itself. The normalization of the prior function is chosen such that the area under it coincides with the integral over the mock spectral function. The frequency range  $\omega \in [-10, 20]$  is divided into  $N_\omega = 1500$  points whereas  $\tau \in [0, 6.1]$  with  $N_\tau = 12$  unless stated otherwise. To capture the large dynamical range of the Kernel, resulting from the inclusion of negative frequencies, the internal arithmetic is set to use 384 bits of precision.

### A. Search space basis

In this subsection we would like to investigate the effects of the choice of search space on the final reconstructed function  $\rho$ . To separate the question of successful reconstruction from the quality of data, we use a small noise  $\eta = 0.0001$  to only slightly distort the ideal mock data. We restrict ourselves to a small number of data-points as it is exactly these cases where in practice the prescription of Bryan fails.

According to Fig.2 and Fig.3 we find that from this small dataset we can only reconstruct the lowest lying peak at positive frequencies reliably. The error bars shown are obtained solely from the estimated curvature of the  $\mathcal{Q}$  functional using the submatrix approximation. All higher lying structures show a large amount of variation when changing

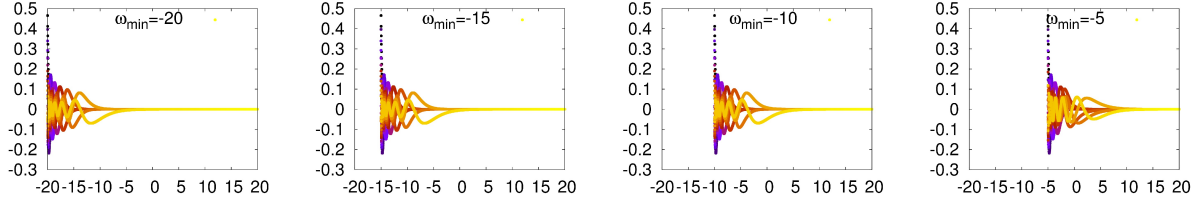


FIG. 5. The basis vectors of Bryan’s search space for different  $\omega_{\min}$  and constant  $\Delta\omega = 0.02$ .

between different basis sets. Note that the lowest lying peak is also only reconstructed well for the cases where we use an extended search space of  $N^{\text{ext}} > 32$ . For smaller sets of basis vectors even the lowest positive peak appears significantly broadened and diminished in height.

This behavior can be understood by looking at the available basis functions explicitly in Fig.4. Based on Bryan’s prescription we obtain twelve different functions, shown in the left panel of the first row. We find that they exhibit very few variation for positive frequencies, which in turn leads to the absence of sharp peak structures in the reconstruction. The larger the basis gets the more we find oscillating behavior in individual functions that then allows for a better reconstruction of the sharp lowest lying peak.

Note that Bryan’s definition does also not take into account the choice of the frequency interval. In Fig.5 we show the behavior of the basis functions under a change of  $\omega_{\min}$ , while keeping the resolution fixed  $\Delta\omega = \frac{\omega_{\max} - \omega_{\min}}{N_{\omega}} = \text{const}$ . Since the number of data-points does not change we are left with the same twelve functions each time, which as we see are only shifted towards smaller frequencies. It is clear that in the case of  $\omega_{\min} = -20, -15$  no structures remain on the positive frequency side and thus reconstruction of sharp peak structures is becoming increasingly difficult.

Another indicator for the success of the method is the reproduction of the supplied dataset by  $D^p$ . The MEM differs from the pure  $\chi^2$  fitting in that its aim is not the pure minimization of the functional  $\mathcal{L}$  but taking also into account the constraints from the entropy part  $\mathcal{S}$ . Nevertheless a successful MEM reconstruction needs to be able to reproduce the provided dataset within its errors. However if we take a look at the result using Bryan’s prescription in Fig.6 (the left panel of the first row), we can clearly see that the data-points between  $4.5 < \omega < 6$  are not reproduced within their small errors. This leads to a large value of  $\mathcal{Q}$  where  $\mathcal{L} \gg \mathcal{S}$ . Only when we go to larger search spaces will  $\mathcal{L}$  and

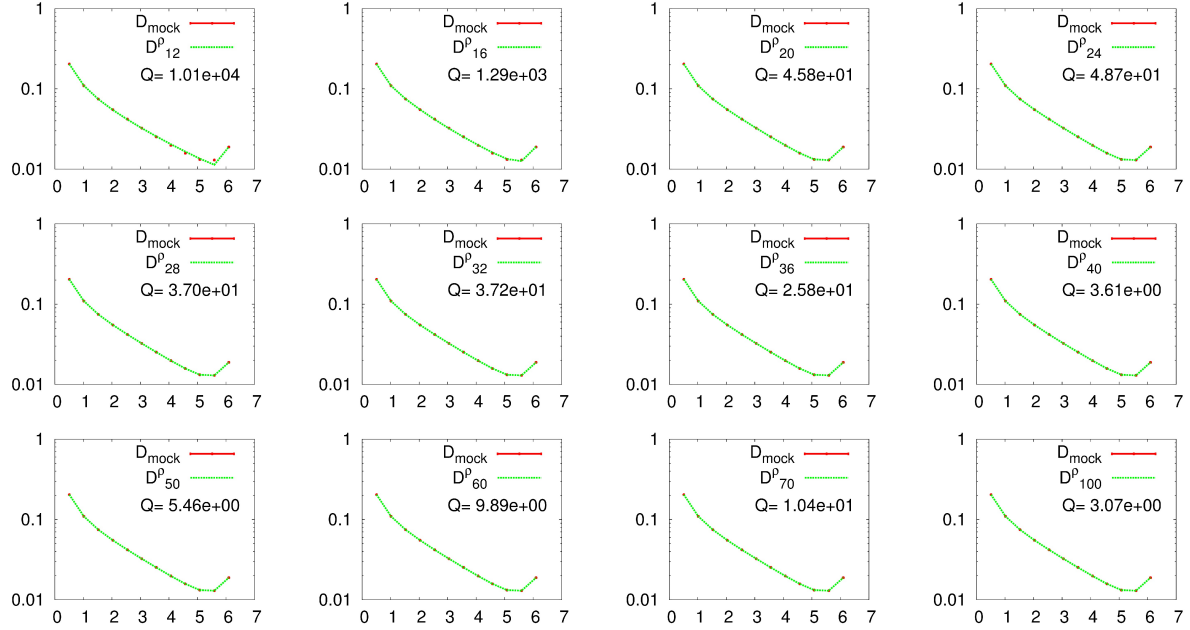


FIG. 6. Comparison of the data  $D^{\text{mock}}$  generated from the mock function  $\rho_{\text{mock}}$  and the data corresponding to the MEM reconstruction  $D^p$ . The values for  $Q$  are taken at the value of  $\alpha$  at which  $P[\alpha|D, I(m)]$  takes its maximum.

thus  $Q$  decrease such that it actually becomes of the order of magnitude of  $S$  after which it does not decrease significantly anymore.

## B. Quality of data

As has been pointed out in previous MEM studies, e.g. in [5], the success of the reconstruction depends crucially on the quality of the supplied data. In Fig.7 we show the result of a mock data run for different strengths of the noise parameter  $\eta$ . Note that for smaller noise the results improve, however the shown error bars, coming from the curvature of the  $Q$  functional alone, do not reliably capture the deviation of e.g. the second peak position. (see the center and right panel for  $\eta = 0.01, 0.001$ ).

## V. MONTE CARLO DATA ANALYSIS

Since the mock data is initialized with uncorrelated noise we use real-world lattice QCD data to take a more realistic look at the previously mentioned issues of error esti-

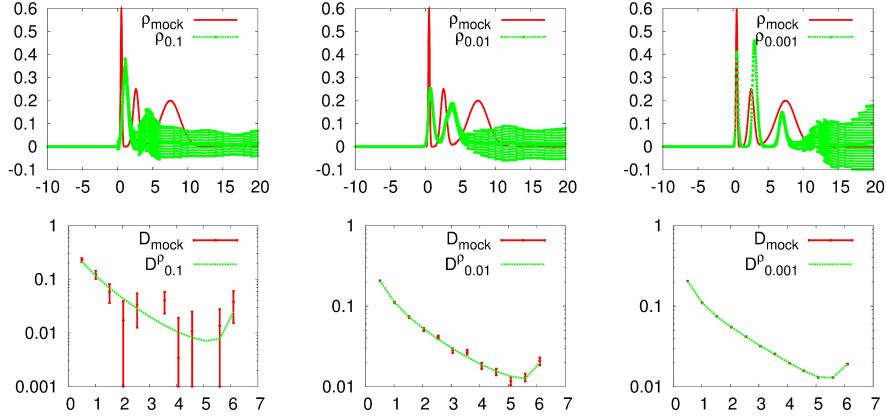


FIG. 7. Reconstruction of the mock function  $\rho_{\text{mock}}$  for different strengths  $\eta$  of noise applied to the mock data.

mation. We use data from the study of a quantity called the Wilson loop[8]. (The data is obtained from a Monte Carlo simulation of quenched lattice QCD based on the naive Wilson plaquette action on a  $\xi_{\text{ren}} = 4$  anisotropic hypercube with  $N_x = 20$ ,  $N_\tau = 12$  and lattice spacings  $\beta = 6.1$  translating to  $a_s = 0.097\text{fm}$  in physical units).

Using a total number of  $N_{\text{conf}} = 1490$  measurements of the simulated quantity, we find from Fig.8 that even though the encoded peaks appear to be broader compared to the mock data case, we have to go to at least  $N^{\text{ext}} = 24$  before the double peak content of the lowest lying structure is starting to be resolved.

Using this result we can also see the benefit of varying the prior function as a means of systematic error estimation, as mentioned in subsection III D. In Fig.10 ( $N^{\text{ext}} = 36$ ) the double peak content of the lowest lying structure is relatively stable against variation of the prior function over four orders of magnitude. The small peaks for  $3 < \omega < 10$  on the other hand vary significantly both in position and width. This tells us that these smaller structures are not constrained by the data but instead are an artifact introduced by the particular choice of the prior function. (Note that these smaller structures only appear after increasing the number of basis function beyond  $N^{\text{ext}} > 24$ .)

As a last issue we would like to see how the choice of the length of the error intervals for Eq.(41) affects the actual value of the errors obtained. Furthermore we ask whether the approximation of the inverse of the error matrix by the local submatrix significantly changes the outcome of the calculation.

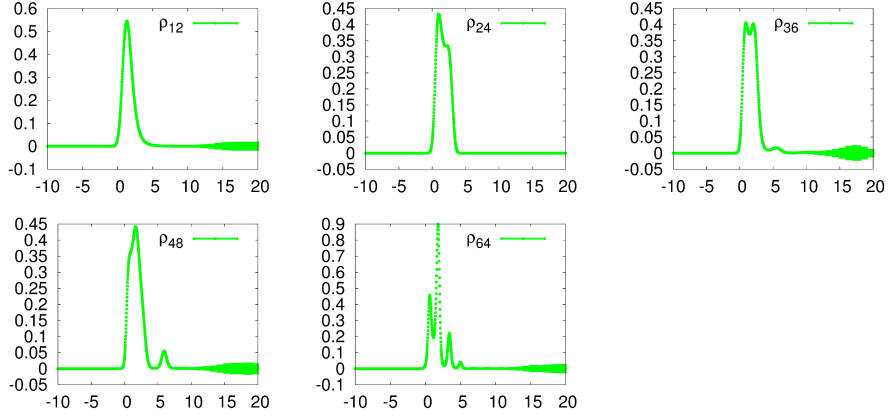


FIG. 8. Reconstruction of the function  $\rho$  based on a dataset from quenched Lattice QCD for different values of  $N^{\text{ext}}$ .

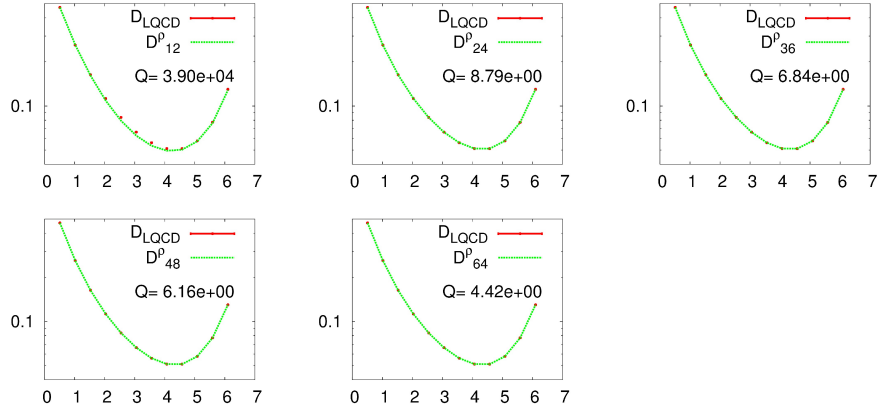


FIG. 9. The lattice QCD data underlying the reconstruction in Fig.8 compared to the data corresponding to the MEM reconstruction.

Fig.11 tells us that choosing too long intervals, in the above e.g. the case  $N_{\text{err}} = 5$ , the resulting errors are not reliable, since they crudely both over and underestimate the values obtained from finer spaced calculations. It is interesting to note that increasing the number of intervals does not seem to make the error smaller in size so that it converges toward a continuous function.

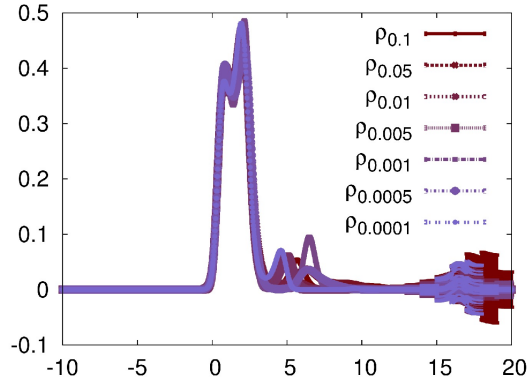


FIG. 10. Identification of artifacts (in this case the structures at  $3 < \omega < 10$ ) in the function  $\rho$  introduced by increasing the number of basis vectors  $N^{\text{ext}} = 36 > N_{\tau} = 12$ . The relative stability of the lowest two peaks indicate them being constrained by the data while all other features vary strongly with the amplitude of  $m(\omega)$

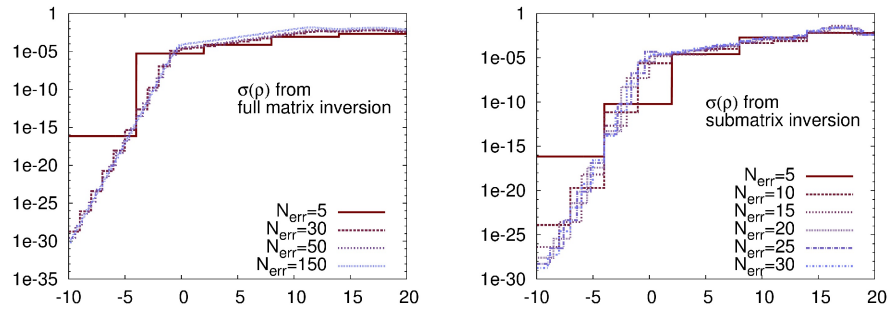


FIG. 11. Comparison of the influence of the number of error intervals  $N_{\text{err}}$  on the value of the estimated error. (left) Errors obtained from the inversion of the full error matrix in Eq.(40) (right) Errors from the inversion of only submatrices.

## VI. CONCLUSION

The Maximum Entropy method offers a solution to the question of how to bring meaning to the ill-defined problem (1) of inferring the function  $\rho(\omega)$  from a noisy and finite dataset  $D(\tau)$ . Instead of maximizing only the likelihood probability with a test spectral function  $\rho(\omega)$ , we are asked to include explicitly all our prior knowledge of the system in form of the prior function  $m(\omega)$  that enters the prior probability. The function  $\rho^{\text{MEM}}(\omega)$  that represents the extremum of (17) is hence the most probable answer in the Bayesian sense.

Both conceptual arguments on the handling of prior information and the numerical examples in section 3 are the basis for our claim that the global maximum of (17) does in general not lie in the image of transpose of the Kernel  $K$  from (1). Thus restricting the search for  $\rho^{\text{MEM}}$  to Bryan's subspace does in general not allow a reliable reconstruction. In a quest to still limit the dimensionality of the search space for the global maximum of (17) a priori, we proposed an systematic extension of the search space in Eq.(41) with dimensionality  $N_{\text{ext}} > N_{\tau}$ .

Introducing a large number of basis functions will inevitably lead to the appearance of "wiggly" structures in the final reconstructed function  $\rho^{\text{MEM}}(\omega)$ . Since they are however not constrained by the data, such artifacts can be identified by a variation of the prior function. Those features of  $\rho^{\text{MEM}}(\omega)$  that are reliably encoded in the data on the other hand do not suffer strongly from such variations.

### A. Recipe for a consistent MEM

1. Measure the data points with as small error as possible.
2. Construct the best possible prior function  $m_l$  that contains all known information about the system.
3. Search for the global maximum of  $P[\rho|Dm]$ .
  - Either use the (L-)BFGS algorithm to directly maximize in  $N_{\omega}$  variables, OR
  - Start with Bryan's search space and increase the number of basis vectors according to Eq.(25) until the maximum value of  $Q(\rho)$  determined by the maximizing algorithm does not increase anymore.

4. For the spectral structures obtained in this way carry out the determination of the intrinsic error according to Eq.(41).
5. Repeat from 3. after changing the prior function in amplitude and if possible also shape.
6. By identifying those spectral features that remain unchanged under the variation of the prior and that show small errors from step 4., locate the structures that are truly constrained by the data.

The author would like to thank O.Kaczmarek and S. Sasaki for the many valuable discussions and comments. A.R. acknowledges support from the BMBF project *Heavy Quarks as a Bridge between Heavy Ion Collisions and QCD* as well as funding from the Sofja Kovalevskaja program of the Alexander von Humboldt foundation and the EU Integrated Infrastructure Initiative *Hadron Physics 2*

- 
- [1] A. Rothkopf, *ExtMEM (Maximum Entropy Method with an extended search space)* (2011), source code and manual available at <http://www.scicode.org/ExtMEM>, <http://www.scicode.org/ExtMEM>.
  - [2] E. T. Jaynes, in *SIAM-AMS Proceedings* (McLaughlin, 1984) pp. 151–166, <http://bayes.wustl.edu>.
  - [3] R. Bryan, *European Biophysics Journal* **18**, 165 (1990), ISSN 0175-7571, 10.1007/BF02427376, <http://dx.doi.org/10.1007/BF02427376>.
  - [4] M. Jarrell and J. Gubernatis, *Physics Reports* **269**, 133 (1996), ISSN 0370-1573, <http://www.sciencedirect.com/science/article/pii/0370157395000747>.
  - [5] M. Asakawa, T. Hatsuda, and Y. Nakahara, *Prog.Part.Nucl.Phys.* **46**, 459 (2001), arXiv:hep-lat/0011040 [hep-lat].
  - [6] D. Nickel, *Annals Phys.* **322**, 1949 (2007), arXiv:hep-ph/0607224 [hep-ph].
  - [7] W. H. Press, S. A. Teukolsky, W. T. Vetterling, and B. P. Flannery, *Numerical Recipes 3rd Edition: The Art of Scientific Computing*, 3rd ed. (Cambridge University Press, New York, NY, USA, 2007) ISBN 0521880688, 9780521880688.
  - [8] A. Rothkopf, T. Hatsuda, and S. Sasaki(2011), arXiv:1108.1579 [hep-lat].